Abstract

Background:

Microdialysis (MD) is conventionally used to measure the *in vivo* levels of various substances and metabolites in extracellular and cerebrospinal fluid of brain. However, insertion of the MD probe and subsequent perfusion to obtain samples cause damage in the vicinity of the insertion site, raising questions regarding the validity of the measurements.

New Method:

We used fluorogenic derivatization liquid chromatography-tandem mass spectrometry, that quantifies both high and low abundance proteins, to differentiate the effects of perfusion from the effects of probe insertion on the proteomic profiles of expressed proteins in rat brain.

Results:

We found that the expression levels of five proteins were significantly lower in the perfusion group than in the non-perfusion group. Three of these proteins are directly involved in ATP synthesis. In contrast to decreased levels of the three proteins involved in ATP synthesis, ATP assays show that perfusion, following probe insertion, even for a short time (3 h) increased ATP level up to 148% that prior to perfusion, and returned it to normal state (before probe insertion).

Comparison with Existing method

There is essentially no information regarding which observed changes are due to probe insertion and which to perfusion.

Conclusions:

Our findings partially demonstrate that the influence of whole MD sampling process may not significantly compromise brain function and subsequent analytical results may have physiological equivalence to normal, although energy production is transiently damaged by probe insertion.

Introduction

Microdialysis (MD) is an established technique for the *in vivo* sampling of various substances in the extracellular fluid and cerebrospinal fluid of the brain and is conducted to obtain precise information about the dynamics and extracellular concentrations of neurotransmitters or drugs transferred into the brain. However, implanting MD probes into the brain causes immediate tissue injury and disruption of the blood-brain barrier (BBB), activation of microglia and astrocytes, inflammation, loss of oxygen perfusion, and neural degeneration (Kozai, 2016). Thus, several intervention strategies to minimize damage caused by probe implantation have been proposed, including miniaturizing probe devices and the retrodialysis of dexamethasone (Kozai, 2016; Nebsitt, 2015). These approaches can reduce the artificial influence of neural implants and return metabolic reactions to their normal state. However, compared to the effect of probe implantation, little attention has been paid to the influence of artificial cerebral spinal fluid (aCSF) perfusion conducted after probe implantation to collect target substances in brain tissue.

Perfusion in MD is generally performed at flow rates of ~2 μL/min. Inflammatory responses resulting in the release of inflammatory mediators such as chemokines and cytokines are triggered by probe implantation (Stenken 2010; Jaquins-Gerstl 2011) and can be spread throughout the brain by perfusion in MD. Therefore, reducing the damage caused by aCSF perfusion is important to perform MD sampling in a state as similar to normal as possible. For this purpose, it is necessary to understand the influence of perfusion itself on brain function with distinguishing this

influence from tissue damage caused by probe implantation.

Electrophysiological methods, *in vivo* imaging and biological approaches have been used to investigate the mechanism and the cascade of tissue damage induced by MD sampling (Kozai, 2016). However, it remains unknown how the proteome profile in brain changes due to such tissue damage, although the up- or down-regulation of proteins directly reflects MD-associated events and brain function. Fluorogenic derivatization liquid chromatography-tandem mass spectrometry (FD-LC-MS/MS) is a proteomic method. This method involves a multi-step process: the fluorogenic derivatization of proteins, followed by LC of the derivatized proteins, the isolation of proteins that are differentially expressed in the various treatment groups, enzymatic digestion of the isolated proteins, and identification of the isolated proteins via LC-MS/MS using a database-search algorithm (Masuda, 2004). The applicability of the method has been demonstrated in the analyses of extracts from *Caenorhabditis elegans*, mouse liver/heart/stomach, breast cancer cell lines, and thoroughbred horse skeletal muscle, revealing the proteins related to early stage Parkinson's disease, hepatocarcinogenesis /drug-induced cardiotoxicity/drug-induced gastric ulcers, metastatic breast cancer, and training effects, respectively (Ichibangase, 2012; Ohyama, 2010; Ohyama, 2012). FD-LC-MS/MS can be used to analyze a complex proteome sample containing both high- and low-abundance proteins because these peaks are easily distinguished in the same chromatogram. Furthermore, this method enables the highly sensitive detection of very low-abundance proteins at the femtomole level because a non-fluorescent reagent is used to yield highly fluorescent products with an

ultra-low signal-to-noise baseline on the chromatogram. MD-induced damage and its influence on subsequently obtained analytical results have long been recognized but never been adequately addressed, and comprehensive understanding this damage is important to researchers who regularly use MD sampling as a tool in analysis of various substances in brain.

The present study aimed to understand how the proteome profile changes due to MD trauma induced solely by aCSF perfusion. We performed proteomic analyses of MD-injured rat brain tissue collected immediately after insertion of an MD probe and after 3-h perfusion (2 μL/min) following probe insertion. In accordance with the proteomic findings, we performed ATP assays for the brain tissues collected at different timings (before and after perfusion, before probe-insertion) to understand the influence of perfusion on energy production during MD sampling.

Material and methods

MD procedure

Rats were anesthetized with three types of mixed anesthetic agents (medetomidine hydrochloride 0.15mg/kg, midazolam 2.0 mg/kg, butorphanol tartrate 2.5 mg/kg intraperitoneally (i.p.)) and fixed on a stereotaxic system (SR-5R, Narishige Scientific Instrument, Tokyo). A CMA microdialysis system (Carnegie Medicine, Stockholm, Sweden) was used. Microdialysis probe with a 2-mm, 50 kDa cutoff artificial cellulose membrane (Eicom, Kyoto, Japan) was implanted in the left striatum (coordinates: A, +0.6 mm; L, +3.0 mm from bregma; H, −7.0 mm from the skull surface) (Paxinos and

Watson, 2007) and was perfused with aCSF at a flow rate of 2.0 μl/min in the perfusion group. All of aCSF prepared with analytical grade reagents consisted of KCl 2.5 mM, NaCl 125 mM, $MgCl \cdot 6H_2O$ 1.0 mM, $NaHPO_4 \cdot 2H_2O$ 0.5 mM, $NaH_2PO_4 \cdot 12H_2O$ 2.5 mM, and $CaCl_2$ 1.2 mM. Brains were removed 3 hours after insertion of the probe in the non-perfusion group (n=5) and 3 hours after the start of perfusion in the perfusion group (n=5). In addition, for ATP assay, brain tissues were also collected before perfusion, as control, or after 3-h perfusion at 0.5 μL/min. All animal experiments were performed of Nagasaki University and were approved by the Institutional Animal Care and Use Committee of Nagasaki University (approval number: 140419-1-2).

Tissue treatment

Each whole brain tissue tissue was frozen at -196 °C and was immediately homogenized using the Frozen Cell Crasher (Microtec Co. Ltd, Chiba, Japan). Each sample of homogenized brain tissue (50 mg) was suspended in 250 μl of 10 mM 3-[(3-cholamidopropyl)-dimethylammonio] propanesulfonate (CHAPS) solution (Dojindo Laboratories, Kumamoto, Japan), and the homogenates were centrifuged at 5000 *g* for 15 min at 4 °C. The supernatant of each sample was then collected and stored as the soluble fraction at -80 °C until use. The total protein content of each supernatant sample was determined using the Quick Start Bradford Protein assay kit (Bio-Rad Laboratory, Hercules, CA, USA) and bovine serum albumin as a protein standard according to the manufacturer's instructions. After determination of total protein content in the soluble fractions, the supernatant was diluted with CHAPS solution to a

concentration of 5.0 mg total protein/ml and used as a starting protein sample.

FD-LC-MS/MS

Briefly, a 10-µl volume of sample was mixed with a mixture of tris(2-carboxyethyl)phosphine hydrochloride, ethylenediamine-*N*,*N*,*N'*,*N'*-tetraacetic acid, and CHAPS in guanidine hydrochloride buffer solution. Then, this sample was subsequently mixed with 5 µl of 140 mM 7-chloro-*N*-[2-(dimethylamine)ethyl]-2,1,3-benzoxadiazole-4-sulfonamide, which is the fluorogenic derivatization reagent, in acetonitrile. After the reaction mixture was incubated in a 50°C water bath for 5 min, 3 µl of 20% trifluoroacetic acid was added to stop the derivatization reaction. A portion (20 µl) of this reaction mixture (8.7 µg protein) was injected into the HPLC-fluorescence detection system at a flow rate of 0.6 ml/min. The protein column (Intrada WP-RP) was used as a stationary phase for separation of the derivatized proteins at a column temperature of 60°C. Corresponding peak heights were compared to identify differential protein profiles in the two groups.

Each subject protein in eluent recovered from the above HPLC system was concentrated to 5 µl under reduced pressure and used for further identification process. The residue was diluted with ammonium bicarbonate solution (pH 7.8), calcium chloride, and 20 ng/µl trypsin, and the resultant mixture was incubated for more than 6 h at 37°C. This mixture was then concentrated to 20 µl under reduced pressure.

Each peptide mixture was subjected to an LC-electrospray ionization-tandem mass spectrometer. The sample was loaded onto a precolumn (300 µm i.d. x 5.0 mm,

L-C-18, Chemicals and Evaluation and Research Institute) in the injection loop and washed using 0.1% TFA in 2% acetonitrile. Peptides were separated and ion-sprayed into MS by a packed spray capillary column (C18, 75 μm i.d. x 125 mm, Nano HPLC Capillary Column) with a spray voltage from 1.5 to 2.5 kV. The mass spectrometer was configured to optimize the duty cycle length with the quality of data acquired by progressing from a full scan of the sample to three tandem MS scans of the three most intense precursor masses (as determined by Xcaliber® software [Thermo Fisher Scientific] in real time). MS/MS data were extracted using Proteome Discoverer 1.2 (Thermo Fisher Scientific). Spectra were searched against a rat subdatabase from the public non-redundant protein database (Swiss-Prot). The filter criteria (single, double, and triple charge peptides with a correlation factor [XCorr] and protein probability [P]) were adjusted maintaining the empirically determined protein false discovery rate less than 5%. False discovery rate was calculated using the number of significant unique peptide in the reversed database divided by the number of those in the forward database. More details of the analytical method can be found in supplementary data.

LC fractionation followed by tryptic digestion and MS/MS analysis were performed using the top of each peak. Finally, the proteins detected by duplicate or triplicate MS/MS analyses were selected as an identified protein.

ATP measurement

ATP levels were measured in homogenated brain tissue (100 mg) for control, perfusion (0.5 and 2.0 μL/min) and non-perfusion groups. A chemiluminescent method using

luciferin-luciferase was employed to determine ATP concentrations. ATP was extracted from homogenates in 10 mM HEPES-NaOH with 0.25 M sucrose. Samples were assayed using the ATP assay kit (TA100, Toyo Ink., Tokyo, Japan) and a Sirius Luminometer (Berthold Japan, Tokyo), according to the manufacturer's protocol.

Statistical analysis

Differences in peak heights between perfusion and non-perfusion groups, and differences in ATP levels between perfusion (2.0 μL/min), perfusion (0.5 μL/min), non-perfusion and control groups and between left (probe-insertion) and right (non-probe insertion) sides of brains were determined by unpaired Tukey Kramer multiple comparison test using JMP sofware. $P < 0.05$ was considered to be significant.

Results

Typical FD-LC chromatograms of rat brain samples from the perfusion and non-perfusion groups are depicted in Fig. 1. The total amount required for quantification was 8.7 μg per HPLC injection. The precision of the method was confirmed based on the reproducibility of the peak heights using three peaks, including early eluting (5.24%), medium eluting (5.93%) and late eluting (14.9%) peaks in chromatogram for between-days (n=3) replicates. The reproducibility of the retention times using same peaks was also calculated, and the between-day CV were less than 1.48% (n=3).

The height of each peak indicates the expression level of an individual protein. The expression levels of five proteins differed significantly between the two groups (*P*

182 < 0.05; Table 1) and the peaks representing these proteins are numbered in Fig. 1. Each
183 differentially expressed protein was expressed less in the perfusion group than in the
184 non-perfusion group.

185 The brain ATP levels were assessed using a chemiluminescent ATP assay (Fig.
186 2), as described in the "Materials and Methods" section. The ATP concentrations in the
187 brain tissues of the perfusion and non-perfusion groups were 13.5±2.2 nmol/g and
188 9.1±1.1 nmol/g, respectively. The ATP concentration after 3-h perfusion (2.0 μL/min)
189 significantly increased to 148% that prior to perfusion ($P < 0.05$, n = 5). We also
190 performed the ATP assay for brain tissues collected before MD probe insertion (control)
191 or after probe insertion and 3-h perfusion at 0.5 μL/min. Furthermore, the brain tissues,
192 collected after 3-h perfusion at 0.5 μL/min, were separated at the center into two pieces;
193 left side (probe insertion side) and right side (the other side without insertion) were
194 subjected to compare ATP levels between the two sides. The ATP concentrations were as
195 follows: 13.4±3.2 nmol/g (control); 15.2±1.6 nmol/g (perfusion at 0.5 μL/min);
196 15.3±3.4 nmol/g (left side, probe insertion side); 15.0±4.0 nmol/g (right side, non-probe
197 insertion side). Comparing the concentrations between before and after probe insertion
198 without perfusion (*i.e.*, control (13.4±3.2 nmol/g) *versus* non-perfusion group (9.1±1.1
199 nmol/g)), probe insertion itself significantly reduce ATP concentration to 68% that prior
200 to insertion ($P < 0.05$). However, the ATP concentrations of brain tissues collected after
201 perfusion at 0.5 or 2.0 μL/min were same as control (Fig. 2; $P = 0.60$ or 1.00,
202 respectively). Also, ATP concentration at the probe insertion side (left side, 15.3±3.4
203 nmol/g) was same as that of the other side (right side, 15.0±4.0 nmol/g).

Discussion

Implanting an MD probe causes traumatic penetration injury to brain tissue that triggers ischemia, decreases glucose metabolism, opens the BBB, activates astrocytes and microglia, damages neurons, axons and terminals, and leads to scar formation at the probe track (Benvensite, 1987; Clapp-Lilly, 1999; Zhou, 2002; Tang, 2003; Varner, 2016). Despite this tissue disruption, MD has successfully been used to monitor brain neurochemistry in many application studies. Acute and chronic tissue damage occurs in response to the insertion of the probe and subsequent aCSF perfusion. Local disturbance associated with the trauma of probe implantation is likely to influence the study outcome; consequently, several groups have tried to quantify and calculate the extent of physiological damage to correct the study outcome (Clapp-Lilly, 1999; Tang, 2003; Stenken, 2010). However, the invasive nature of any brain sampling technique cannot avoid penetration injury caused by probe implantation, even when a small probe is used or dexamethasone is administered post-perfusion. Therefore, minimizing the influence of the perfusion process on brain function is important to obtain data in a state as similar to normal as possible.

Numerous studies have focused on the influence of probe insertion, whereas only one study have dealt with the influence of aCSF perfusion in MD (Clapp-Lilly, 1999). Light microscope analysis revealed tissue disruption up to 1.4 mm from the probe site, and qualitative ultrastructural analysis found swollen mitochondria and bloated endoplasmic reticulum around the same site, leading to intracellular chemical

disruption (Clapp-Lilly, 1999). This tissue damage was induced by perfusion because it occurred distant from the probe. This study shows an association between perfusion and tissue damage in MD sampling; however, there has been little investigation of the tissue response to perfusion, and the effect of perfusion alone on damage or response of the tissue has never been evaluated to distinguish this damage from that caused by probe insertion. Since it is unclear how perfusion influences brain function and what kind of influence occurs, flow rates cannot be optimized to reduce tissue physiological and functional change.

Proteomics is a promising approach for understanding the damage induced by perfusion because it provides information on dynamic cellular performance derived from the comprehensive analysis of gene expression at the protein level. Of the proteomics approaches currently available, the FD-LC-MS/MS method detects minor proteins at sub-fmol amounts and allows the direct comparison of the levels of both abundant and minor proteins from the same chromatogram. Each of the five differentially expressed proteins noted above was expressed less in the perfusion group than in the non-perfusion group (Fig. 1, Table 1). The differentially expressed proteins identified in our study are involved in ATP synthesis or in the cytoskeletal network: ATP synthase subunit *E* (peak 2), glyceraldehyde-3-phosphate dehydrogenase (GAPDH, peak 4), and malate dehydrogenase (peak 5) are involved in ATP synthesis, and cofilin-1 (peak 1) and coactocin-like protein (peak 3) are involved in the cytoskeletal network.

In the present study, we observed decreased levels of the three proteins involved in ATP synthesis via ATP synthase, the glycolytic pathway or the TCA cycle in

248 rat brain following aCSF perfusion. Therefore, we assessed ATP levels in the two
249 groups (perfusion and non-perfusion) using a chemiluminescent ATP assay kit (Fig. 2).
250 The ATP level in the perfusion group was 148% that of the non-perfusion group,
251 suggesting that depression of ATP synthase subunit *E*, GAPDH and malate
252 dehydrogenase does not lead to an ATP decrease, although the levels of other enzymes
253 involved in ATP synthesis did not change. This result was fully unexpected and
254 stimulated us to perform further ATP assay for brain tissues collected before probe
255 insertion, as control, or after 3-h perfusion at a lower flow rate (0.5 μL/min) than 2.0
256 μL/min to examine how much influence probe insertion itself and flow rate have on
257 ATP level. Among non-perfusion, perfusion (2.0 μL/min), perfusion (0.5 μL/min) and
258 control groups, the ATP concentration after probe insertion (non-perfusion group) was
259 significantly reduced to 68% that prior to insertion (control), and those in perfusion
260 groups were not significantly different from that in control group (Fig. 2). Probe
261 insertion reduced ATP level as expected, while the perfusion may positively acts in ATP
262 synthesis, given that the ATP concentration after 3-h perfusion returned to that before
263 probe insertion. Furthermore, the significant ATP decrease due to probe insertion may
264 be repaired by perfusion because its level at the probe-inserted side (left side) was same
265 as that of the other side (right side). Also, the effect of perfusion on ATP concentration
266 did not depend on the flow rate, given that there was no difference of ATP levels
267 between flow rates of 0.5 and 2.0 μL/min (Fig. 2). It has been reported that MD probe
268 insertion may induce glucose hypermetabolism and may depress glucose levels
269 (Benvensite, 1987; Sumbria, 2011; Groothuis, 1998; Morgan, 1996). This

hypermetabolism can increase ATP levels and may occur as a response to ATP reduction induced by MD probe insertion. However, in our proteomic study, up-regulated enzymes involved in glycolysis pathway were not found; therefore, the ATP increase by perfusion cannot be explained.

The brain requires a large amount of energy to sustain its contractile performance; consequently, the depression of ATP levels should strongly influence brain function. In addition, extracellular ATP regulates microglial branch dynamics in the intact brain, and the release of ATP from damaged tissue and surrounding astrocytes mediates a rapid microglial response towards injury (Davalos, 2005). Therefore, the ATP increase by perfusion positively affects the process for spontaneously rescuing brain injury and recovering brain function. Since the stock of ATP in the brain is small, a perfusion-induced increase in ATP synthesis would likely result in recovered brain function. BBB opening induced by probe insertion has been reported to be transient and to be largely repaired within 1.5 h after probe insertion (Sumbria, 2011). Therefore, aCSF perfusion may accelerate such repairmen and may recover the ATP level to be in a state as similar to normal. Perfusion in MD sampling has been reported to induce intracellular disruption, such as swollen mitochondria and bloated endoplasmic reticulum (Clapp-Lilly, 1999). The present study suggests that perfusion-induced tissue damage may not lead to reduced brain function. Our findings partially demonstrate that, owing to the positive effect of perfusion, MD sampling does not significantly compromise brain function and that subsequent analytical results have physiological equivalence to normal from the perspective of energy. Our finding may ensure that 3-h

perfusion recoveries ATP depression induced by probe-insertion and the period is needed for normalization. This is supported by the initial studies finding that glucose metabolism and blood flow decreased within three hours following probe implantation but these changes were seen 24 h after the implantation (Benveniste, 1987). On the other hand, considering that there was no significant difference in ATP level between 2.0 and 0.5 μL/min, 45-min perfusion at 2.0 μL/min may effectively and time-consumingly recover ATP depression if perfusion volume is important for the ATP recovery. Our finding may not be applied to the case in a long-time MD sampling (e.g. 24 hour). For the case, ATP profile within such a long time after probe-insertion and perfusion start will be required to finally conclude an optimal normalization period.

The present study also reveals that two actin-related proteins associated with the cytoskeleton are significantly reduced in the perfusion group compared with the non-perfusion group. Cofilin is best known as a regulator of actin filament non-equilibrium assembly and disassembly. Whether cofilin promotes actin assembly or disassembly depends on the concentration of cofilin relative to actin and the relative concentrations of other actin-binding proteins (Bernstein, 2010; Van Troys, 2008). In addition, cofilin modulates actin filament branching, chaperons actin to the nucleus, translocates actin to mitochondria, and opens the mitochondrial permeability transition pore. Coactosin-like protein works as an actin binding protein and is a member of the ADF/cofilin group (de Hostos, 1993). In this study, the levels of two actin-related proteins were significantly depressed in the perfusion group and interestingly, both proteins are reported to be associated with the ADF-cofilin complex (Bernstein, 2010,

de Hostos, 2013). A reduction in actin dynamics is thought to cause a decrease in mitochondrial membrane potential and an increase in the levels of reactive oxygen species (Gourlay, 2005).

Conclusion

To date there has been only one report of how the proteome profile changes due to the acute trauma caused by MD, and that report studied the trauma caused by probe insertion into the human trapezius muscle (Turkina, 2017). Therefore, the present study is the first to comprehensively investigate the effect of perfusion following probe insertion into the brain using a proteomic approach. We found that three enzymes involved in ATP synthesis significantly decreased after 3-h perfusion. However, despite down-regulation of the three enzymes, ATP assays show that the perfusion even for a short time (3 h) increased ATP levels up to 148% that prior to perfusion, and returned it to its normal state (before probe insertion). Our findings partially demonstrate that the influence of whole MD sampling process may not significantly compromise brain function and widely-performed analysis of samples obtained by MD may have physiological equivalence to normal, although energy production is transiently damaged by probe insertion.

References

Bernstein, B.W., Bamburg, J.R., 2010. ADF/Cofilin: a functional node in cell biology. Trends Cell Biol. 20, 187-195.

Benvensite, H., Drejer, J., Schousboe, A., Diemer, N.H., 1987. Regional cerebral glucose phosphorylation and blood-flow after insertion of a microdialysis fiber through the dorsal hippocampus in the rat. J. Neurochem. 49, 729-734.

Clapp-Lilly, K.L., Roberts, R.C., Duffy, L.K., Irons, K.P., Hu, Y., Drew, K.L., 1999. An ultrastructural analysis of tissue surrounding a microdialysis probe. J. Neurosci. Methods 90, 129-142.

Davalos, D., Grutzendler J., Yang, G., Kim, J.V., Zuo, Y., Jung, S., Littman, D.R., Dustin, M.L., Gan, W.B., 2005. ATP mediates rapid microglial response to local brain injury in vivo. Nat. Neurosci. 8, 752-758.

de Hostos, E.L., Bradtke, B., Lottspeich, F., Gerisch, G., Coactosin, 1993. a 17 kDa F-actin binding protein from Dictyostelium discoideum. Cell Motil. Cytoskeleton 26, 181-191.

Gourlay, C.W., Ayscough, K.R., 2005. Indentification of an upstream regulatory pathway controlling actin-mediated apoptosis in yeast. J. Cell Sci. 118, 2119-2132.

Groothuis, D.R., Wardbc, S., Schlageterabc K.E., Itskovichbc, A.C., Schwerinbc, S.C., Allena, C.V., Dillsd, C., Levycd, R.M., 1998. Changes in blood-brain barrier permeability associated with insertion of brain cannulas and microdialysis probe. Brain Res. 803, 218-230.

Ichibangase, T., Imai., K., 2012. FD-LC-MS/MS for determining protein expression and

355 elucidating biochemical events in tissues and cells. Biol. Pharm. Bull. 35, 1393-1400.
356 Jaquins-Gerstl, A., Shu, Z., Zhang, J., Liu, Y., Weber, S.G., Michael, A.C., 2011. Effect
357 of dexamethasone on gliosis, ischemia, and dopamine extraction during microdialysis
358 sampling in brain tissue. Anal. Chem. 83, 7662-7667.
359 Kozai, T.D.Y., Jaquins-Gerstl, A.S., Vazquez, A.L., Michael, A.C., Cui, X.T., 2016.
360 Dexamethasone retrodialysis attenuates microglial response to implanted probes in vivo.
361 Biomaterials 87, 157-169.
362 Masuda, M., Saimaru, H., Takamura, N., Imai, K., 2004. Fluorogenic derivatization
363 reagents suitable for isolation and identification of cystein-containing proteins utilizing
364 high-performance liquid chromatography-tandem mass spectrometry. Anal. Chem. 76,
365 728-735.
366 Morgan, M.E., Singhal, D., Anderson, B.D., 1996. Quantitative assessment of
367 blood-brain barrier damage during microdialysis. Pharmacol. Exp. Ther. 277,
368 1167-1176.
369 Nebsitt, K.M., Varner, E.L., Jaquins-Gerstl, A., Michael, A.C., 2015. Microdialysis in
370 the rat striatum: Effects of 24 h dexamethasone retrodialysis on evoked dopamine
371 release and penetration injury. ACS Chem. Neurosci. 6, 163-173.
372 Ohyama., K., Tomonari, M., Ichibangase, T., To, H., Kishikawa, N., Nakashima, K.,
373 Imai, K., Kuroda, N., 2010. A toxicoproteomic study on cardioprotective effects of
374 pre-administration of docetaxel in a mouse model of adriamycin-induced cardiotoxicity.
375 Biochem. Pharmacol. 80, 540-547.
376 Ohyama, K., Shiokawa, A., Ito, K., Masuyama, R., Ichibangase, T., Kishikawa, N., Imai,

377 K., Kuroda, N., 2012. Toxicoproteomic analysis of a mouse model of nonsteroidal
378 anti-inflammatory drug-induced gastric ulcers. Biochem. Biophys. Res. Commun. 420,
379 210-215.
380 Paxinos, G., Watson, C., 2007. The rat brain in stereotaxic coordinates, seven ed.,
381 Academic Press, Cambridge.
382 Stenken, J.A., Church, M.K., Gill, C.A., Clough, G.F., 2010. How minimally invasive is
383 microdialysis sampling? A cautionary note for cytokine collection in human skin and
384 other clinical studies. AAPS J. 12, 73-78.
385 Sumbria, R.K., Klein, J., Bickel, U., 2011. Acute depression of energy metabolism after
386 microdialysis probe implantation is distinct from ischemia-induced changes in mouse
387 brain. Neurochem. Res. 36, 109-116.
388 Tang, A., Bungay, P.M., Gonzales, R.A., 2003. Characterization of probe and tissue
389 factors that influence interpretation of quantitative microdialysis experiments for
390 dopamin. J. Neurosci. Methods 126, 1-11.
391 Turkina, M.V., Ghafouri, N., Gerdle B., Ghafouri, B., 2017. Evaluation of dynamic
392 changes in interstitial fluid proteome following microdialysis probe insertion trauma in
393 trapezius muscle of healthy women. Sci. Rep. 7, 43512.
394 Varner, E.L., Jaquins-Gerstl A., Michael, A.C., 2016. Enhanced intracranial
395 microdialysis by reduction of traumatic penetration injury at the probe track. ACS Chem.
396 Neurosci. 7, 728-736.
397 Van Troys, M., Huyck, L., Leyman, S., Dhaese, S., Vandekerkhove, J., Ampe, C., 2008.
398 Ins and outs of ADF/cofilin activity and regulation. Eur. J. Cell Biol. 87, 649-667.

399 Zhou, F., Braddock, J.F., Hu, Y., Zhu, X., Castellani R.J., Smith, M.A., Drew, K.L.,
400 2002. Microbial origin of glutamate, hibernation and tissue trauma: an in vivo
401 microdialysis study. J. Neurosci. Methods 119, 121-128.
402

403 **Figure captions**

404

405 **Fig. 1** Chromatograms of proteins derivatized with DAABD-Cl in rat brain. The
406 upper and lower chromatograms were obtained from the perfusion and non-perfusion
407 groups, respectively. The peaks resulting from differentially expressed proteins are
408 numbered.

409

410 **Fig. 2** Comparison of ATP concentrations between control (before probe-insertion),
411 non-perfusion and perfusion (at 2.0 μL/min, at 0.5 μL/min) groups. Significant
412 differences between the groups are indicated by $*P \leq 0.05$ or $**P \leq 0.01$.

Fig. 1

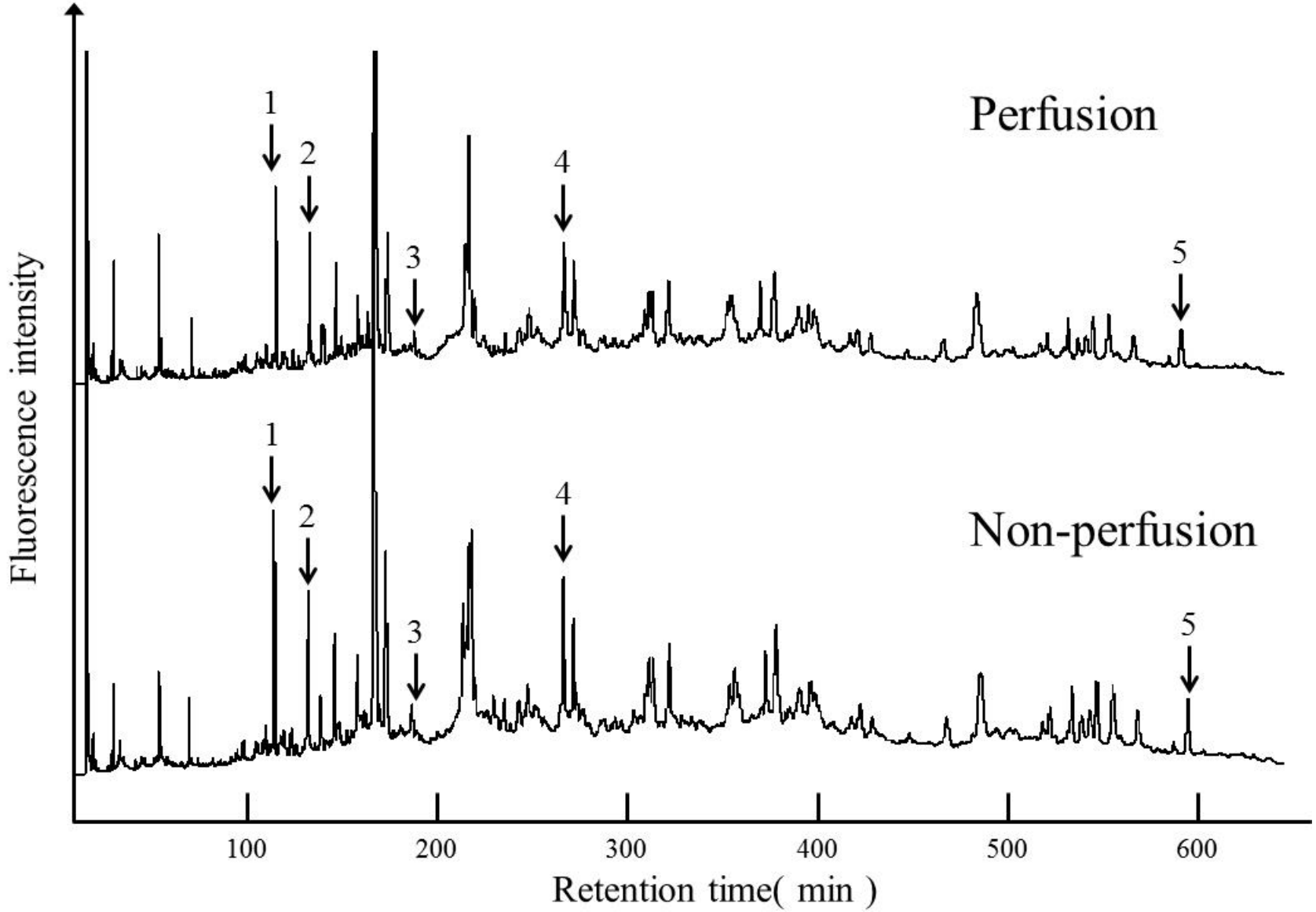
Perfusion
Non-perfusion
1
2
3
4
5
Fluorescence intensity
100
200
300
400
500
600
Retention time(min)

Fig. 2

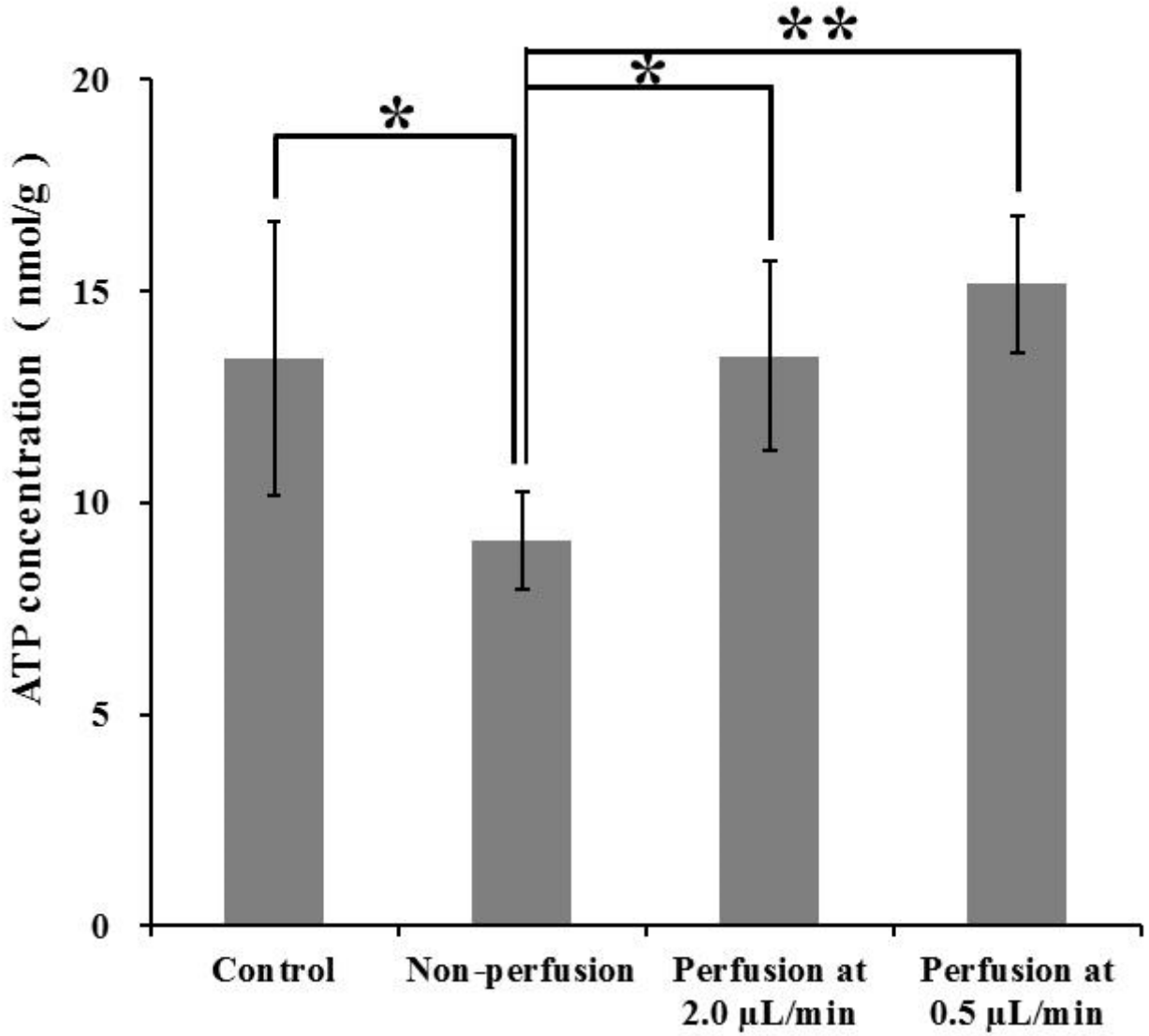
**
*
*
ATP concentration (nmol/g)
20
15
10
5
0
Control
Non-perfusion
Perfusion at 2.0 µL/min
Perfusion at 0.5 µL/min

Table 1 List of proteins identified using the FD-LC-MS/MS method

Peak number[a)]	Protein name	Perfusion/non-perfusion ratio[b)]	Score[c)]	Coverage[d)]	Unique peptides[e)]	Accession[f)]
1	Cofilin-1	0.64	18.65	43.98	5	P45592
2	ATP synthase subunit e, mitochondrial	0.78	6.68	21.13	2	P29419
3	Coactosin-like protein	0.58	4.51	10.56	2	B0BNA5
4	Glyceraldehyde-3-phosphate dehydrogenase	0.69	19.12	14.71	3	P04797
5	Malate dehydrogenase, cytoplasmic	0.75	13.01	14.97	4	O88989

[a)]Peak numbers correspond to those in Fig. 1. [b)] Perfusion/non-perfusion ratio: the ratio of the amount of a protein in the perfusion group relative to that in the non-perfusion group. [c)] The protein score is the sum of all peptide Xcorr values (SEQUEST search algorithm). [d)] The percent coverage is calculated by dividing the number of amino acids in all found peptides by the total number of amino acids in the entire protein sequence. [e)] The number of peptide sequence unique to a protein group. [f)] Accession number number is simply a series of digits that are assigned consecutively to each sequence record processed by Swiss-prot.